$(CO)_2)_2(OEP)]$, A. Takenaka, Y. Sasada, H. Ogoshi, T. Omura, and Z. Yoshida, *ibid.*, **31**, 1 (1975); $[(H_4OEP)^{2+}(Rh(CO)_2Cl_2)^-{}_2]$, E. Cetinkaya, A. W. Johnson, M. F. Lappert, G. M. McLaughlin, and K. W. Muir, *J. Chem. Soc., Dalton Trans.*, 1236 (1974).

(10) (a) ++,++,++,++ for H_2(*N*-carbethoxymethyl-OEP)$^+$, G. M. McLaughlin, *J. Chem. Soc., Perkin Trans. 2*, 136 (1974); $H_3(OEP)^+$, N. Hirayama, A. Takenaka, Y. Sasada, E. Watanabe, H. Ogoshi, and Z. Yoshida, *J. Chem. Soc., Chem. Commun.*, 330 (1974); [Ti(5,15-Me_2-5,15-H_2-OEP)(O)], P. N. Dwyer, L. Puppe, J. W. Buchler, and W. R. Scheidt, *Inorg. Chem.*, **14**, 1782 (1975); $(H_3OEP)^+[Re_2Cl_3(CO)_6]^-$, C. P. Hrung, M. Tsutsui, D. L. Cullen, and E. F. Meyer, Jr., *J. Am. Chem. Soc.*, **98**, 7878 (1976). (b) ++,++,++,+− for [Co(*N*-(ethyl acetate)-OEP)(Cl)], D. E. Goldberg and K. M. Thomas, *ibid.*, **98**, 913 (1976). (c) ++,++,+−,−− for [Co(OEP)(1-Me-Im)] (Im = imidazole), R. G. Little and J. A. Ibers, *J. Am. Chem. Soc.*, **96**, 4452 (1974). (d) ++,+−,++,+− for [Ni(5,15-Me_2-5,15-H_2-OEP)], P. N. Dwyer, J. W. Buchler, and W. R. Scheidt, *ibid.*, **96**, 2789 (1974). (e) ++,+−,−−,−+ for $[Fe(OEP)(Im)_2]$, A. Takenaka, Y. Sasada, E. Watanabe, H. Ogoshi, and Z. Yoshida, *Chem. Lett.*, 1235 (1972). (f) ++,−+,−−,+− for $[Ru(OEP)(py)_2]$, F. R. Hopf, T. P. O'Brien, W. R. Scheidt, and D. G. Whitten, *J. Am. Chem. Soc.*, **97**, 277 (1975). (g) ++,−−,++,−− for tetragonal [Ni(OEP)], E. F. Meyer, Jr., *Acta Crystallogr., Sect. B*, **28**, 2162 (1972).

(11) D. M. Collins, R. Countryman, and J. L. Hoard, *J. Am. Chem. Soc.*, **94**, 2066 (1972).

(12) R. G. Little, K. R. Dymock, and J. A. Ibers, *J. Am. Chem. Soc.*, **97**, 4532 (1975).

(13) J. R. Sams, personal communication.

Contribution from the Department of Chemistry, University of Wisconsin,
Madison, Wisconsin 53706

Synthesis, X-ray Crystal Structure, and Temperature-Dependent NMR Spectrum of Tetraethylammonium (α-Methoxybenzyl)pentacarbonyltungstate

CHARLES P. CASEY,* STANLEY W. POLICHNOWSKI, HENDRIK E. TUINSTRA, LOREN D. ALBIN, and JOSEPH C. CALABRESE

Received May 4, 1978

The reaction of $(CO)_5WC(OCH_3)C_6H_5$ with $K^+HB[OCH(CH_3)_2]_3^-$ followed by cation exchange with $N(CH_2CH_3)_4^+Br^-$ gives $N(CH_2CH_3)_4^+(CO)_5WCH(OCH_3)C_6H_5^-$, **3**, which is the precursor of $(CO)_5WCHC_6H_5$. **3** was characterized spectrally and by single-crystal X-ray diffraction. **3** crystallizes in the monoclinic system, space group $P2_1/c$. The unit cell constants are $a = 12.908$ (6) Å, $b = 11.663$ (6) Å, $c = 16.875$ (9) Å, $\beta = 111.60$ (4)°, and $Z = 4$. The final discrepancy indices are $R_1 = 3.55\%$ and $R_2 = 4.31\%$ for the 2941 independent reflections having $I \geq 2\sigma(I)$ in the range $3° \leq 2\theta \leq 45°$. The temperature-dependent NMR of the closely related compound $N(CH_2CH_3)_4^+(CO)_5WCH(OCH_3)[C_6H_3\text{-}3,5\text{-}(CH_3)_2]^-$, **5**, indicates that there is a barrier to rotation ($\Delta G^{\ddagger} = 8.7$ kcal) about the aryl–benzylic carbon bond of **5**.

Introduction

$(CO)_5WC(C_6H_5)_2$ reacts with alkenes to give cyclopropanes, olefin scission products, and new carbene complexes.[1] A mechanistic scheme involving the equilibrium between a metallacyclobutane and a metal complex bearing both an alkene and a carbene ligand was proposed to explain these results. Earlier, a similar equilibration had been suggested by Herrisson and Chauvin[2] as a sufficient mechanism for the olefin metathesis reaction.[3] The recent demonstration that the olefin metathesis reaction proceeds via a nonpairwise exchange of alkylidene groups is consistent with the equilibration between a metallacyclobutane and a metal complex bearing both carbene and alkene ligands and excludes mechanisms requiring the pairwise exchange of alkylidene groups of a pair of alkenes complexed to a metal.[4]

Earlier we pointed out that the moderate stereospecificity observed in the metathesis of 2-pentenes[5] can be explained in terms of the formation of the more stable puckered metallacyclobutane in which repulsive, 1,3-diaxial interactions are minimized.[6,7] In addition, the puckered metallacyclobutane hypothesis predicts the preferential formation of cis cyclopropanes from the reaction of a "large–small" carbene complex with a 1-alkene.[6]

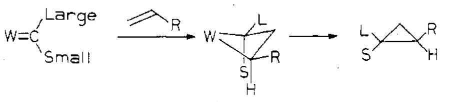

Our initial attempts to test the puckered metallacyclobutane hypothesis were frustrated by the rapid decomposition of $(CO)_5WC(C_6H_5)CH_3$ via facile β-hydride elimination from the methyl group.[6] In another attempt to test the puckered metallacyclobutane hypothesis, we set out to prepare $(CO)_5WC(C_6H_5)H$, **1**, which could not undergo decomposition by β-hydride elimination. A two-step synthesis of **1** from $(CO)_5WC(OCH_3)C_6H_5$, **2**, was developed. Reduction of **2** with $K^+HB[OCH(CH_3)_2]_3^-$ gave the key intermediate $N(CH_2CH_3)_4^+(CO)_5WCH(OCH_3)C_6H_5^-$, **3**.[8] Protonation of **3** with CF_3CO_2H at −78 °C gave the desired phenylcarbene complex **1** which was observed by ^1H NMR at −78 °C but which decomposes rapidly at −50 °C.[8] The reactions of **1** with alkenes to give cyclopropanes will be the subject of a future paper. In this paper, we report the synthesis, X-ray crystal structure, and temperature-dependent NMR spectrum of the key intermediate, $N(CH_2CH_3)_4^+(CO)_5WCH(OCH_3)C_6H_5^-$, **3**. These findings represent the first data available on the bonding and conformational preferences in alkylpentacarbonyltungsten compounds.

Results and Discussion

Synthesis. Since nucleophiles attack metal carbene complexes at the carbene carbon atom, we set out to prepare $(CO)_5WCH(OCH_3)C_6H_5^-$ by hydride addition to arylmethoxycarbene complexes. Addition of potassium triisopropoxyborohydride,[9] **4**, to a red solution of $(CO)_5WC(OCH_3)C_6H_5$, **2**, in THF at 0 °C gave a light yellow solution. Addition of aqueous tetraethylammonium bromide followed by evaporation of THF gave an 86% yield of $N(CH_2CH_3)_4^+(CO)_5WCH(OCH_3)C_6H_5^-$, **3**, as a bright yellow solid which was further purified by recrystallization from CH_2Cl_2 at −20 °C. This reduction could also be accomplished with $Na^+HB(OCH_3)_3^-$[10] but this proved to be less convenient since the later reagent decomposed at a moderate rate even when stored at −20 °C. Reduction of $(CO)_5WC(OCH_3)C_6H_5$ with $NaBH_4$ was briefly investigated by NMR; the production of $(CO)_5WCH_2C_6H_5^-$[11] and of $(CO)_5WHW(CO)_5^-$ was

0020-1669/78/1317-3045$01.00/0

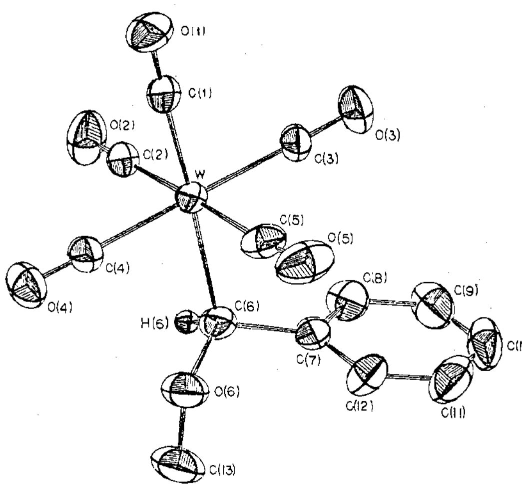

Figure 1. Structure of **3** (cation omitted) with thermal ellipsoids of 30% probability.

observed by NMR. Previously, Fischer reported that the reduction of $(CO)_5WC(OCH_3)C_6H_5$ by sodium methoxide in methanol gave **3** in 9% yield.[12]

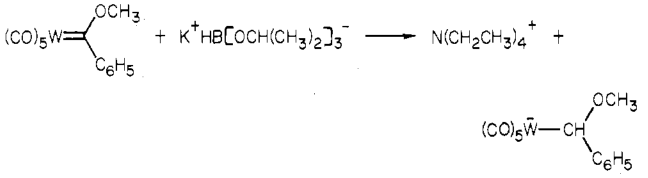

$$(CO)_5W{=}C(OCH_3)(C_6H_5) + K^+HB[OCH(CH_3)_2]_3^- \longrightarrow N(CH_2CH_3)_4^+ + (CO)_5\bar{W}{-}CH(OCH_3)(C_6H_5)$$

3 is moderately air sensitive in the solid state and is rapidly decomposed by air in solution. The infrared spectrum of **3** consisting of four bands at 2036 (w), 1935 (w), 1892 (s), and 1841 (m) cm^{-1} is very similar to that of other $(CO)_5W{-}R^-$ species.[11] In the ^1H NMR spectrum of **3**, the benzylic proton absorbs at δ 4.88 with satellite peaks due to a 5.9 Hz coupling to ^{183}W (spin $^1/_2$, 14% natural abundance). The para proton on the phenyl ring of **3** appears as a multiplet at δ 6.56 shifted upfield from the ortho and meta protons which appear as a multiplet centered at δ 7.02. Similar chemical shifts and splitting patterns were observed previously for $N(CH_3)_4^+(CO)_5WCH_2C_6H_5^-$.[11]

The reduction of $(CO)_5WC(OCH_3)[C_6H_3\text{-}3,5\text{-}(CH_3)_2]$ with $Na^+HB(OCH_3)_3^-$ gave $N(CH_2CH_3)_4^+(CO)_5WCH(OCH_3)[C_6H_3\text{-}3,5\text{-}(CH_3)_2]^-$, **5**, which was used in NMR studies described below. In addition, $N(CH_2CH_3)_4^+(CO)_5WCH(OCH_3)[C_6H_2\text{-}2,4,6\text{-}(CH_3)_3]^-$, $N(CH_2CH_3)_4^+(CO)_5WCH(OCH_3)C_6H_4\text{-}p\text{-}CH_3^-$, and $N(CH_2CH_3)_4^+(CO)_5WCH(OCH_3)C_6H_4\text{-}p\text{-}OCH_3^-$ were prepared by similar routes.

In view of the analogy often made between carbene complexes and organic esters,[13] it is somewhat surprising that there have been few reports of reactions of carbene complexes with metal hydride reagents. The reduction of an amino-substituted carbene complex with $LiAlH_4$ results in the overall cleavage of the carbene ligand from the metal to give the corresponding amine in unspecified yield.[14]

$$(CO)_5Cr{=}C(NHR)CH_3 + LiAlH_4 \rightarrow CH_3CH_2NHR$$

The reaction of $(CO)_5CrC(OCH_3)CH_3$ with $LiAl(O\text{-}t\text{-}Bu_3)H$ gave a <0.1% yield of $(CO)_5CrC(OCH_3)CH{=}CHCH{=}C(OCH_3)CH_3$.[15] The failure of these alkyl-substituted carbene complexes to undergo clean reduction might be related to side reactions arising from deprotonation of the acidic protons on the carbon α to the carbene carbon atom.[16] It should be pointed out that clean reductive cleavage of the carbene ligand from metal carbene complexes can be achieved by uncatalyzed reaction with hydrogen.[17]

Table I. Bonding Distances (Å) for $NEt_4^+(CO)_5WCH(OCH_3)C_6H_5^-$

W–C(1)	1.97 (1)	C(7)–C(8)	1.38 (1)
W–C(2)	2.03 (1)	C(8)–C(9)	1.37 (1)
W–C(3)	2.01 (1)	C(9)–C(10)	1.35 (1)
W–C(4)	2.03 (1)	C(10)–C(11)	1.36 (2)
W–C(5)	2.03 (1)	C(11)–C(12)	1.35 (1)
W–C(6)	2.34 (1)	C(12)–C(7)	1.38 (1)
C(1)–O(1)	1.17 (1)	N–C(14)	1.51 (1)
C(2)–O(2)	1.14 (1)	N–C(16)	1.50 (1)
C(3)–O(3)	1.15 (1)	N–C(18)	1.51 (1)
C(4)–O(4)	1.16 (1)	N–C(20)	1.51 (1)
C(5)–O(5)	1.14 (1)	C(14)–C(15)	1.49 (1)
C(6)–O(6)	1.43 (1)	C(16)–C(17)	1.49 (2)
C(13)–O(6)	1.42 (1)	C(18)–C(19)	1.49 (1)
C(6)–C(7)	1.51 (1)	C(20)–C(21)	1.50 (1)

Table II. Intramolecular Bond Angles (deg) for $NEt_4^+(CO)_5WCH(OCH_3)C_6H_5^-$

C(1)–W–C(2)	91.9 (4)	W–C(6)–C(7)	111.5 (5)
C(1)–W–C(3)	90.3 (3)	C(6)–O(6)–C(13)	112.5 (8)
C(1)–W–C(4)	90.7 (3)	O(6)–C(6)–C(7)	111.3 (6)
C(1)–W–C(5)	92.5 (4)	C(6)–C(7)–C(8)	119.8 (8)
C(1)–W–C(6)	177.3 (3)	C(6)–C(7)–C(12)	122.7 (8)
C(6)–W–C(2)	88.6 (3)	C(7)–C(8)–C(9)	120.5 (10)
C(6)–W–C(3)	92.4 (3)	C(7)–C(12)–C(11)	120.9 (10)
C(6)–W–C(4)	86.6 (3)	C(8)–C(9)–C(10)	120.9 (11)
C(6)–W–C(5)	87.1 (3)	C(9)–C(10)–C(11)	119.0 (10)
C(2)–W–C(5)	175.2 (3)	C(10)–C(11)–C(12)	121.2 (11)
C(2)–W–C(4)	91.6 (3)	C(8)–C(7)–C(12)	117.5 (8)
C(2)–W–C(3)	88.1 (3)	N–C(14)–C(15)	115.9 (9)
C(4)–W–C(3)	178.9 (3)	N–C(16)–C(17)	116.9 (10)
C(4)–W–C(5)	90.4 (4)	N–C(18)–C(19)	117.1 (8)
C(5)–W–C(3)	89.8 (4)	N–C(20)–C(21)	116.6 (8)
W–C(1)–O(1)	178.5 (7)	C(14)–N–C(16)	112.5 (7)
W–C(2)–O(2)	178.8 (7)	C(14)–N–C(18)	107.3 (7)
W–C(3)–O(3)	177.1 (8)	C(14)–N–C(20)	111.2 (7)
W–C(4)–O(4)	178.5 (7)	C(16)–N–C(18)	112.4 (7)
W–C(5)–O(5)	176.9 (7)	C(16)–N–C(20)	105.0 (7)
W–C(6)–O(6)	109.4 (5)	C(18)–N–C(20)	108.3 (7)

X-ray Crystal Structure. The X-ray crystal structure of **3** shown in Figure 1 was determined by standard heavy-atom techniques and refined to $R_1 = 0.035$ and $R_2 = 0.043$. The structure of **3** consists of an α-methoxybenzyl ligand and five carbonyl ligands octahedrally coordinated to tungsten (Tables I and II). The benzylic carbon(6)–tungsten bond length of **3** is 2.34 (1) Å. The carbon–metal bond distance in this W(0) compound is somewhat longer than the 2.28 (1)-Å benzylic carbon–metal bond in the W(IV) compound **6**[18] and longer than the 2.20 (5)-Å methyl–tungsten bond in the W(VI) compound $W(CH_3)_4[ON(CH_3)NO]_2$.[19] The metal–carbon single bond distance in **3** is longer than the 2.14 (2)-Å tungsten-carbon double bond of $(CO)_5WC{=}C(C_6H_5)_2$[20] and the 1.90 (5)-Å tungsten–carbon triple bond of $I(CO)_4W{\equiv}CC_6H_5$.[21] The decrease in bond lengths parallels that observed for the hydrocarbon series alkyne < alkene < alkane and is consistent with the proposed multiple bonding of metal carbene and metal carbyne complexes.

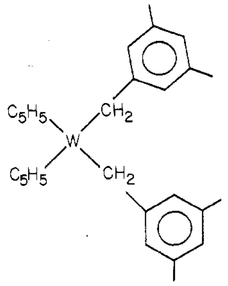

6

The W–C(1) bond distance for the carbonyl ligand trans to the benzyl group in **3** is 0.06 Å shorter than the average

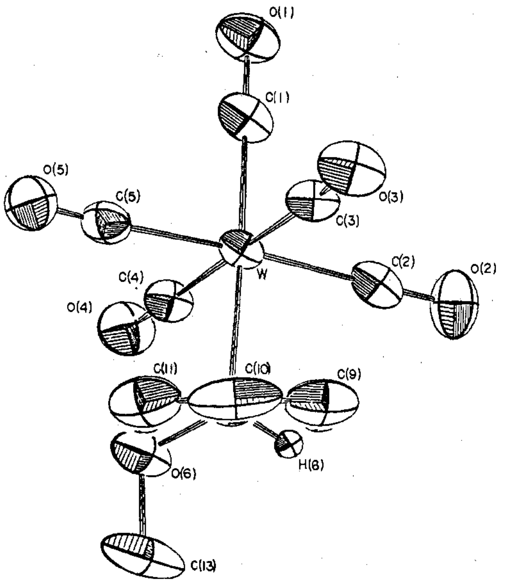

Figure 2. Structure of $(CO)_5WCH(OCH_3)C_6H_5^-$, **3**, viewed down the C(10)–C(7)–C(6) axis with thermal ellipsoids of 30% probability.

of the cis W–C distances. The shorter W–C(1) distance is consistent with a greater degree of back-bonding to the trans CO. The fact that the infrared absorption for the trans CO (A′, mode) occurs at lower frequency than the absorptions due to the cis CO's in **3** is also consistent with the structural data.

As shown in Figure 2, the W–C(6)–C(7) plane is nearly perpendicular (86.5°) to the plane of the phenyl ring. This arrangement minimizes the steric interactions between the $W(CO)_5$ fragment and the phenyl ring. At the same time, this arrangement puts the W–C(6) bond into conjugation with the π system of the phenyl ring. This could allow electron density to be shifted from the carbon–metal bond into the phenyl ring. A shift of electron density by this mechanism may account for the anomalous upfield NMR chemical shift of the para proton in **3**.

Temperature-Dependent NMR. NMR spectra of **3** were recorded at various temperatures between 25 and −90 °C in connection with work on the generation of $(CO)_5WCHC_6H_5$ from **3** and acid. At temperatures below −60 °C a significant broadening occurred in the phenyl region of the NMR even though other absorptions in the spectrum remained sharp. Although this effect was readily attributed to the "freezing out" of the rotation about the phenyl ring–benzylic carbon single bond, the observation of a substantial barrier appeared unusual for a phenyl ring with no ortho substituents. Since the barrier is presumably the result of the pentacarbonyltungsten moiety, a measurement of the activation for the rotation in this and other similar compounds would give a quantitative indication of the steric size of the pentacarbonyltungsten unit and allow comparisons with data available from other studies.

While the ortho protons on the phenyl ring of **3** exhibited a noticeable coalescence point in the low-temperature NMR spectra, band-shape analysis was complicated by coupling of the ortho protons with the meta protons and by the close proximity of the ortho and meta chemical shifts. To circumvent these difficulties, the temperature dependence of the NMR spectrum of **5** was studied. The ortho protons of **5** constitute a simple two-site exchange system. The para proton of **5** provides an internal standard for the peak heights and widths of the ortho protons in the static structure. The temperature dependence of the NMR for **5** in the phenyl region is shown in Figure 3, and the data and calculated activation parameters are given in Table III. The rates were determined by visual comparison of the observed spectra calculated on the basis of two-site, equal population exchange. While it was hoped that the methyl groups in **5** would allow a second measurement of the activation parameters, only minor broadening of the singlet absorption was observed over the temperature range used.

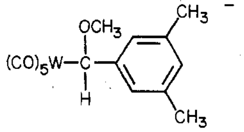

5

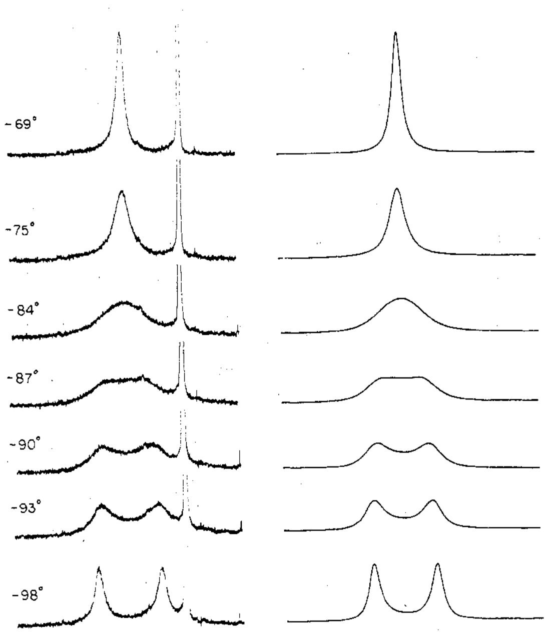

Figure 3. Experimental and simulated temperature-dependent NMR spectra of **5**.

Table III. Activation Parameters from NMR Spectra of **5**

T, °C	k, s^{-1}	activation parameters[a]
−69.1	15.6×10^3	$\Delta G^\ddagger(-84\ °C) = 8.73 \pm 0.04$ kcal/mol
−75.2	7.69×10^2	
−83.9	3.23×10^2	$\Delta H^\ddagger = 7.6 \pm 0.7$ kcal/mol
−87.2	2.27×10^2	
−90.3	1.67×10^2	$\Delta S^\ddagger = -5.7 \pm 3.7$ eu
−93.0	1.25×10^2	
−98.2	0.50×10^2	correlat coeff = −0.9969

[a] 95% confidence limits in the slope and intercept were propagated into the activation parameters.

In qualitative terms, the observed barrier of 8.7 kcal/mol is similar to the $\Delta G^\ddagger$ values obtained for phenyl ring rotation in compounds **7** and **8**.[22,23] For these compounds the activation energies were interpreted in terms of transition states with the sterically large *tert*-butyl group in the plane of the phenyl ring. Similarly, the results of the NMR study of **5** are consistent with a ground state approaching that observed in the X-ray crystal structure and a transition state with the W–C(6) bond coplanar with the phenyl ring. In addition to the unfavorable steric interaction between the tungsten pentacarbonyl unit and the phenyl ring at the transition state, the transition state may also be destabilized relative to the ground state by removing the favorable electronic interaction between the phenyl ring

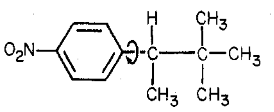

7
$\Delta G^\ddagger = 9.01$ kcal/mol

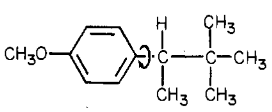

8
$\Delta G^\ddagger = 8.79$ kcal/mol

and the perpendicular carbon–tungsten bond found in the ground state. This interpretation is also consistent with the observation of three methyl singlets for the aryl methyl groups in the NMR spectrum of **9** at about 30 °C. Thus, the ortho

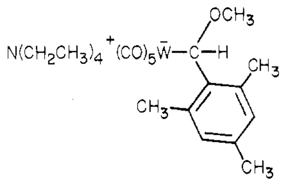

9

substitution in **9** has effectively increased the steric rotation barrier to the extent that rotation of the phenyl ring is not observed at 30 °C.

Experimental Section

$K^+HB[OCH(CH_3)_2]_3^-$, 4, was prepared by a modification of the method of Brown.[9] KH (87.4 mmol; 15 g of a 23.3% mineral oil suspension; Alfa Inorganics) was placed in a Schlenk fritted glass filter maintained under N_2 and washed with several portions of dry hexane to remove the mineral oil. THF (25 mL) was added via syringe, and mixing was effected by bubbling N_2 up through the glass frit. $[(CH_3)_2CHO]_3B$[24] (11 g, 58.5 mmol) was added slowly (to prevent solvent from boiling) and the mixture mixed by N_2 flow for 2 h. The resulting solution of $K^+HB[OCH(CH_3)_2]_3^-$ was separated from excess KH by vacuum filtration overnight and then solvent was removed from the solution under reduced pressure. The resulting oil was heated to 100 °C under vacuum to remove any isopropylborate, cooled, and dissolved in 100 mL of THF. Titration of this solution was accomplished by acidification and measurement of evolved H_2 volumetrically.

$NEt_4^+(CO)_5WCH(OCH_3)C_6H_5^-$, 3. Potassium triisopropoxyborohydride (0.9 M in THF) was added to a solution of $(CO)_5W\text{-}C(OCH_3)C_6H_5$[25] (3.0 g, 6.76 mmol) in 90 mL of THF at 0 °C. An excess of the hydride reagent (1.5–2.2 equiv) was generally required to change the red color of the solution to light yellow, indicating the disappearance of carbene complex. Aqueous 1 M NaOH (30 mL) was added cautiously to destroy excess hydride. Aqueous $N(CH_2CH_3)_4^+Br^-$ (10 mL, 2M, 20 mmol) was then added. A yellow solid precipitated as solvent was removed on a rotary evaporator. The solid was filtered, washed thoroughly with water, and dried in vacuo. Recrystallization was accomplished by dissolving the solid in 10 mL of CH_2Cl_2 in a 40-mL centrifuge tube, centrifuging, transferring the clear solution to another centrifuge tube via cannula, adding hexane (~3.5 mL) until the solution became cloudy, and then adding CH_2Cl_2 until the solution cleared. Cooling to –20 °C gave **3** (3.35 g, 86%) as a moderately air-sensitive yellow crystalline solid. IR (THF) ν_{CO} 2036 (w), 1935 (w), 1892 (s), 1841 (m) cm^{-1}; NMR (acetone-d_6) δ 1.35 (12 H, t of t, J = 7.4, 1.8 Hz), 3.12 (3 H, s), 3.41 (8 H, q, J = 7.4 Hz), 4.88 (1 H, singlet with coupling, $J_{^1H^{183}W}$ = 5.9 Hz, observable as a small doublet centered about the large singlet), 6.56 (1 H, m), 7.02 (4 H, m).

$N(CH_2CH_3)_4^+(CO)_5WCH(OCH_3)[C_6H_3\text{-}3,5\text{-}(CH_3)_2]^-$, 5, was prepared from $Na^+HB(OCH_3)_3^-$[10] and $(CO)_5WC(OCH_3)[C_6H_3\text{-}3,5\text{-}(CH_3)_2]$ in 56% yield by a procedure similar to that used for **3**. IR (THF) 2030 (w), 1939 (m), 1894 (s), 1845 (m) cm^{-1}. NMR (acetone-d_6) δ 1.37 (12 H, t of t, J = 7.4, 1.8 Hz), 2.15 (6 H, s), 3.11 (3 H, s), 3.44 (8 H, q, J = 7.4 Hz), 4.83 (1 H, singlet with additional coupling to ^{183}W), 6.22 (1 H, broad singlet), 6.67 (2 H, broad singlet).

$N(CH_2CH_3)_4^+(CO)_5WCH(OCH_3)[C_6H_2\text{-}2,4,6\text{-}(CH_3)_3]^-$ was prepared from $Na^+HB(OCH_3)_3^-$[10] and $(CO)_5WC(OCH_3)[C_6H_2\text{-}2,4,6\text{-}(CH_3)_3]$ in 44% yield. IR (THF) 2036 (w), 1941 (m), 1890 (s), 1846 (m) cm^{-1}. NMR (acetone-d_6) δ 1.33 (12 H, t of t, J = 7.4, 1.8 Hz), 2.10 (3 H, s), 2.15 (3 H, s), 2.49 (3 H, s), 2.93 (3 H, s), 3.35 (8 H, q, J = 7.4 Hz), 5.18 (1 H, singlet with additional coupling to ^{183}W), 6.46 (2 H, broad singlet).

Crystal Structure Determination. Yellow crystals of **3** suitable for diffraction study were obtained by recrystallization from CH_2Cl_2–hexane at –20 °C. The crystal was mounted on a glass fiber with Elmers glue and sealed in a glass capillary under an argon atmosphere. The crystallographic details are summarized in Table IV.

Table IV. Summary of Crystallographic and X-ray Data for $NEt_4^+(CO)_5WCH(OCH_3)C_6H_5^-$

(a) Crystal Data	
formula	$NEt_4^+(CO)_5WCH(OCH_3)C_6H_5^-$
crystal shape	irregular trapezoid 0.3 × 0.4 × 0.55 mm
cell parameters (errors)[a]	
a, Å	12.908 (6)
b, Å	11.663 (6)
c, Å	16.875 (9)
β, deg	111.60 (4)
cell volume, Å^3	2362
Z	4
d_{calcd}, g/cm^3	1.617
Laue symmetry	monoclinic
space group	$P2_1/c$ [C_{2h}^5, No. 14][26]
systematic absences	$h0l$, $l = 2n + 1$ $0k0$, $k = 2n + 1$
equiv positions	$\pm(x, y, z)$ $\pm(x, {}^1/_2 - y, {}^1/_2 + z)$
(b) Collection and Reduction of the X-ray Diffraction Data	
diffractometer	Syntex $P\bar{1}$[27]
radiation (graphite monochromated)	Mo Kα
range of transmission	0.59–0.74[28]
μ, cm^{-1}	50.26
takeoff angle, deg	4
scan speed (limits), deg/min	2–24
scan range, deg	~2
background: scan time ratio (fixed)	0.67
scan method	θ–2θ
no./freq of std reflectn	2/50
intens variation of std reflectn	±3%
2θ limits, deg	3–45
cutoff of obsd data	$2\sigma(I)$
unique data	2941[29]
P	0.055[29]
(c) Solution and Refinement	
technique of solution	heavy atom
method of refinement	full-matrix least squares[30–32]
isotropic convergence	R_1 = 12.39%, R_2 = 15.26%[33]
isotropic–anisotropic convergence	R_1 = 3.55%, R_2 = 4.31%
max shifts (Δ/σ)	0.05 (x, y, z) 0.05 (B)
error of fit	1.20
data/parameter	2436/262
anomalous dispersion cor	
$\Delta f'$ (real)	–1.421 (W)
$\Delta f''$ (imag)	6.872 (W)
max residual intensity of final diff map, e/Å^3	1.7 (near tungsten); others <0.5

[a] At ambient temperature.

The final positional parameters with estimated errors are listed in Table V. Anisotropic thermal parameters for the nonhydrogen atoms and their estimated errors are listed in Table VI (Supplementary Material). Hydrogen atoms, calculated at C–H distances of 1.00 Å, were assigned constant isotropic thermal parameters of 8.00 Å^2. Bond distances and bond angles are given in Tables I and II, respectively. Table VII (supplementary material) gives the observed and calculated structure factor amplitudes.

Temperature-Dependent NMR of 5. NMR samples were prepared on a vacuum line by distilling degassed acetone-d_6 (0.3 mL) into an NMR tube containing **5** (60–80 mg) and sealing the tube under vacuum.

NMR spectra were recorded on a Bruker WH-270 at 270 MHz. Variable-temperature spectra were obtained using a Bruker cooling device (B-RN$_2$) and controller (B-ST 100/700). Temperatures were measured with a Doric DS-350 instrument (copper–constantan thermocouple, digital readout to 0.1 °C) and are accurate to ±1 °C.

Band-shape analysis was done by visually comparing the observed spectra with simulated spectra calculated on a Wang 7208.[34] The rates obtained by this procedure were used to calculate the activation parameters, assuming a transmission coefficient (K) of 1.0.[36] The activation parameters and confidence limits were determined using a least-squares program incorporating an error propagation calculation.[37]

The near-static NMR spectrum of **5** exhibited absorptions at δ 6.82

Table V. Atom Coordinates for $NEt_4^+(CO)_5WCH(OCH_3)C_6H_5^-$ [a,b]

atom	*x*	*y*	*z*
W	1970.8 (2)	1948.1 (2)	1171.6 (2)
O(1)	1378 (5)	668 (5)	2585 (4)
O(2)	−372 (5)	1345 (6)	−259 (5)
O(3)	884 (5)	4194 (5)	1567 (4)
O(4)	3085 (5)	−319 (5)	794 (4)
O(5)	4292 (5)	2731 (8)	2532 (4)
O(6)	3460 (5)	2319 (5)	93 (4)
N	2383 (5)	6821 (5)	3124 (4)
C(1)	1594 (6)	1131 (6)	2051 (5)
C(2)	475 (6)	1550 (7)	255 (5)
C(3)	1267 (6)	3387 (6)	1400 (5)
C(4)	2681 (6)	511 (7)	921 (5)
C(5)	3466 (6)	2461 (8)	2023 (5)
C(6)	2471 (6)	2845 (7)	123 (5)
C(7)	2627 (6)	4124 (7)	276 (4)
C(8)	1720 (7)	4851 (7)	−39 (5)
C(9)	1836 (9)	5999 (8)	137 (6)
C(10)	2842 (10)	6452 (8)	601 (6)
C(11)	3744 (9)	5751 (9)	885 (6)
C(12)	3650 (7)	4611 (8)	724 (6)
C(13)	3646 (9)	259 (11)	−662 (6)
C(14)	2912 (8)	7970 (8)	3432 (6)
C(15)	3325 (7)	8603 (9)	2837 (6)
C(16)	3159 (7)	6009 (8)	2929 (7)
C(17)	4208 (10)	5701 (11)	3650 (10)
C(18)	1978 (8)	6359 (9)	3792 (5)
C(19)	1502 (9)	5182 (9)	3658 (6)
C(20)	1396 (7)	6936 (7)	2300 (5)
C(21)	489 (8)	7743 (9)	2301 (8)
H(A)	3534	7891	3963
H(B)	2445	8456	3593
H(C)	2826	8500	2266
H(D)	3366	9416	2963
H(E)	4048	8353	2891
H(F)	3373	6319	2483
H(G)	2753	5302	2678
H(H)	4801	5426	3554
H(I)	4460	6355	4071
H(J)	4039	5105	4049
H(K)	1440	6902	3856
H(L)	2564	6434	4341
H(M)	2060	4593	3713
H(N)	1171	4964	4078
H(O)	920	5067	3109
H(P)	1077	6181	2099
H(Q)	1646	7162	1844
H(R)	655	8014	2876
H(S)	412	8372	1940
H(T)	−221	7347	2135
H(1)	4341	2911	−584
H(2)	3582	1883	−1021
H(3)	3067	3089	−1039
H(6)	1867	2720	−430
H(8)	985	4522	−338
H(9)	1116	6520	−97
H(10)	2944	7220	795
H(11)	4490	6102	1202
H(12)	4309	4124	933

[a] *x, y, z,* are fractional coordinates $\times 10^4$. [b] The numbers in parentheses are estimated standard deviations in the last significant digit in this and all other tables.

and 6.39 for the two ortho protons and at δ 6.24 for the para proton on the phenyl ring.

Acknowledgment. This research was supported by the donors of the Petroleum Research Fund, administered by the American Chemical Society, and by the National Science Foundation.

Registry No. 2, 37823-96-4; **3**, 64494-49-1; **4**, 42278-67-1; **5**, 67612-81-1; $(CO)_5WC(OCH_3)[C_6H_3\text{-}3,5\text{-}(CH_3)_2]$, 67612-82-2; $(CO)_5WC(OCH_3)[C_6H_2\text{-}2,4,6\text{-}(CH_3)_3]$, 62342-90-9; $N(CH_2CH_3)_4^+(CO)_5WCH(OCH_3)[C_6H_2\text{-}2,4,6\text{-}(CH_3)_3]^-$, 67612-79-7.

Supplementary Material Available: Table VI, anisotropic thermal parameters, and Table VII, structure factor amplitudes (17 pages). Ordering information is given on any current masthead page.

References and Notes

(1) Casey, C. P.; Burkhardt, T. J. *J. Am. Chem. Soc.* **1974**, *96*, 7808.

(2) Herrisson, J. L.; Chauvin, Y. *Makromol. Chem.* **1970**, *141*, 161. Soufflet, D. C.; Chauvin, Y.; *C. R. Hebd. Seances Acad. Sci., Ser. C* **1973**, *276*, 169.

(3) For reviews of olefin metathesis, see Calderon, N.; Ofstead, E. A.; Judy, W. A. *Angew. Chem., Int. Ed. Engl.* **1976**, *15*, 401. Calderon, N. *Acc. Chem. Res.* **1972**, *5*, 127. Hughes, W. B. *Organomet. Chem. Synth.* **1972**, *1*, 341. Haines, R. J.; Leigh, G. J. *Chem. Soc. Rev.* **1975**, *4*, 155.

(4) (a) Katz, T. J.; McGinnis, J. L. *J. Am. Chem. Soc.* **1975**, *97*, 1592. (b) Grubbs, R. H.; Burk, P. L.; Carr, D. D. *ibid.* **1975**, *97*, 3265. (c) Katz, T. J.; Rothchild, R. *ibid.* **1976**, *98*, 2519. (d) Grubbs, R. H.; Carr, D. D.; Hoppin, C.; Burk, P. L. *ibid.* **1976**, *98*, 3478.

(5) Hughes, W. B. *Chem. Commun.* **1969**, 431. Basset, J. M.; Bilhou, J. L.; Mutin, R.; Theolier, A. *J. Am. Chem. Soc.* **1975**, *97*, 7376.

(6) Casey, C. P.; Albin, L. D.; Burkhardt, T. J. *J. Am. Chem. Soc.* **1977**, *99*, 2533.

(7) A similar analysis of the stereochemistry of olefin metathesis has been advanced: Katz, T. J.; Hersh, W. H. *Tetrahedron Lett.* **1977**, 585.

(8) A preliminary communication has been published.

(9) Brown, C. A. *J. Org. Chem.* **1974**, *39*, 3913.

(10) Brown, H. C.; Mead, E. J.; Trerney, P. A. *J. Am. Chem. Soc.* **1957**, *79*, 5400.

(11) Casey, C. P.; Polichnowski, S. W.; Anderson, R. L. *J. Am. Chem. Soc.* **1975**, *97*, 7375. Casey, C. P.; Polichnowski, S. W. *ibid.* in press.

(12) Fischer, E. O.; Schubert, U.; Kalbfus, W.; Kreiter, C. G. *Z. Anorg. Allg. Chem.* **1975**, *416*, 135.

(13) For recent reviews of transition metal carbene complexes see Fischer, E. O. *Angew. Chem.* **1974**, *86*, 651. Dötz, K. H. *Naturwissenshaftten* **1975**, *62*, 365. Casey, C. P. In "Transition Metal Organometallics in Organic Synthesis", Alper, H., Ed.; Academic Press: New York, 1976; Vol. 1, Chapter 3.

(14) Connor, J. A.; Fischer, E. O. *Chem. Commun.* **1967**, 1024.

(15) Knauss, L.; Fischer, E. O. *J. Organomet. Chem.* **1971**, *31*, C71.

(16) Casey, C. P.; Brunsvold, W. R. *J. Organomet. Chem.* **1976**, *118*, 309, and references therein.

(17) Casey, C. P.; Neumann, S. M. *J. Am. Chem. Soc.* **1977**, *99*, 1651.

(18) Forder, R. A.; Jefferson, I. W.; Prout, K. *Acta Crystallogr., Sect. B*, **1975**, *31*, 618.

(19) Fletcher, S. R.; Shortland, A.; Skapski, A. C.; Wilkinson, G. *J. Chem. Soc., Chem. Commun.* **1972**, 922.

(20) Casey, C. P.; Burkhardt, T. J.; Bunnell, C. A.; Calabrese, J. C. *J. Am. Chem. Soc.* **1977**, *99*, 2127.

(21) Huttner, G.; Lorenz, H.; Gartzke, W. *Angew. Chem., Int. Ed. Engl.* **1974**, *13*, 609.

(22) Anderson, J. E.; Pearson, H.; Rawson, D. I. *J. Chem. Soc., Chem. Commun.*, **1973**, 95.

(23) For a recent review of barriers to rotation about sp^3–sp^2 bonds see Sternhell, S. In "Dynamic Nuclear Magnetic Resonance Spectroscopy", Jackman, L. M., Cotton, F. A., Ed.; Academic Press: New York, 1975.

(24) Brown, H. C.; Mead, E.; Shoaf, C. *J. Am. Chem. Soc.* **1956**, *78*, 3616.

(25) Fischer, E. O.; Massböl, A. *Chem. Ber.* **1967**, *100*, 2445.

(26) "International Tables for X-Ray Crystallography" 2nd ed.; Kynoch Press: Birmingham, England, 1965; Vol. I, p 99.

(27) Sparks, R. A., et al. "Operations Manual. Syntex P$\bar{1}$ Diffractometer", Syntex Analytical Instruments: Cupertino, Calif., 1970.

(28) No correction for absorption was made.

(29) The integrated intensity (I) was calculated according to the expression $I = [S - (B_1 + B_2)/B_R]T_R$ where S is the scan count, B_1 and B_2 are the background counts, B_R is the ratio of background time to scan time, and T_R is the 2θ scan rate in degrees per minute. The standard deviation of I was calculated as $\sigma(I) = T_R[S + (B_1 + B_2)/B_R + (pI)^2]^{1/2}$.

(30) All least-squares refinements were based on the minimization of $\sum w_i \| F_o| - |F_c \|^2$ with the individual weights $w_i = 1/\sigma(F_o)^2$.

(31) Atomic scattering factors used for all nonhydrogens atoms are from Hanson, H. P.; Herman, F.; Lea, J. D.; Skillman, S. *Acta Crystallogr.* **1964**, *17*, 1040. Those for the hydrogen atoms are from Stewart, R. F.; Davidson, E. R.; Simpson, W. T. *J. Chem. Phys.*, **1965**, *43*, 3175.

(32) Programs used in the X-ray structural analysis included ORFLS and ORFEE (Busing, Martin, Levy) for least-squares refinement and error analysis and ORTEP (C. K. Johnson) for molecular plots. Remaining programs were written by J. C. Calabrese.

(33) $R_1 = [\sum \| F_o| - |F_c \| / |F_o|] \times 100\%$ and $R_2 = [\sum w_i \| F_o| - [F_c \|^2 / \sum w_i |F_o|^2]^{1/2}$.

(34) The program used for the simulations was written by Professor H. W. Whitlock utilizing the theory of Gutowsky and Holm.[35] The calculated spectra were plotted on a Wang 712.

(35) Gutowsky, H. S.; Holm, C. H. *J. Chem. Phys.* **1956**, *25*, 1228.

(36) See Binsch, G. *Top. Stereochem.* **1968**, *3*, 122.

(37) The program used for determining the activation parameters and confidence limits[38] was written by G. R. Weisman and run on a Harris computer.

(38) For a discussion of errors in NMR determinations of activation parameters see Binsch, G. In "Dynamic Nuclear Magnetic Resonance Spectroscopy", Jackman, L. M., Cotton, F. A., Ed.; Academic Press: New York, 1975; and references therein.